

Long-range photon-mediated gate scheme between nuclear spin qubits in diamond

Adrian Auer* and Guido Burkard

Department of Physics, University of Konstanz, D-78457 Konstanz, Germany

(Received 30 July 2015; revised manuscript received 4 November 2015; published 4 January 2016)

Defect centers in diamond are exceptional solid-state quantum systems that can have exceedingly long electron and nuclear spin coherence times. So far, single-qubit gates for the nitrogen nuclear spin, a two-qubit gate with a nitrogen-vacancy (NV) center electron spin, and entanglement between nearby nitrogen nuclear spins have been demonstrated. Here, we develop a scheme to implement a universal two-qubit gate between two distant nitrogen nuclear spins. Virtual excitation of an NV center that is embedded in an optical cavity can scatter a laser photon into the cavity mode; we show that this process depends on the nuclear spin state of the nitrogen atom. If two NV centers are simultaneously coupled to a common cavity mode and individually excited, virtual cavity photon exchange can mediate an effective interaction between the nuclear spin qubits, conditioned on the spin state of both nuclei, which implements a universal controlled-Z gate. We predict operation times below $10 \mu\text{s}$, which is four orders of magnitude faster than the decoherence time of nuclear spin qubits in diamond.

DOI: [10.1103/PhysRevB.93.035402](https://doi.org/10.1103/PhysRevB.93.035402)**I. INTRODUCTION**

Substantial experimental progress has been made in demonstrating the viability of nuclear spins coupled to nitrogen-vacancy (NV) centers in diamond as qubits. Compared with the NV electron spin, the nuclear spin offers for superior coherence properties, but so far, a scheme for the necessary two-qubit gates is lacking. Candidate nuclear spins are the intrinsic nitrogen nuclear spin (^{14}N or ^{15}N) [1] or incidental proximal nuclear spins (e.g., ^{13}C) [2]. Decoherence times of $T_2^* \approx 11 \text{ ms}$ at low temperature ($< 10 \text{ K}$) have been measured [3], and elementary single-qubit operations were implemented, including manipulation [1,4–6], initialization [1,4,7–9], and high-fidelity single-shot readout [1,8–11]. It was further demonstrated that the nitrogen nuclear spin can be a functioning part of a small quantum register [3,9,11–14] or can act as a quantum memory to store and later retrieve the NV electron spin state [15]. Nuclear spin entanglement has been studied both experimentally [3,16–19] and theoretically [20–23]. However, a deterministic long-distance coupling scheme that does not utilize prior electron entanglement has not yet been demonstrated. The coupling of nuclear spins is fundamentally required in the context of quantum information processing, e.g., to perform universal quantum computation [24].

In this article, we develop and analyze a mechanism to optically generate a controlled quantum gate between two distant nitrogen nuclear spins (Fig. 1) that works at low temperatures. The coupling between the nuclear spins is achieved by exchanging virtual cavity photons among two NV centers. External laser photons incident on each NV center can be scattered into the cavity mode, or vice versa, by exciting electronic Raman-type transitions between the NV ground and excited state. We find that in the appropriate parameter regime, the scattering process depends on the nitrogen nuclear-spin state and can be completely suppressed for a specific nuclear spin configuration by properly tuning the laser frequency. This nuclear-spin-dependent scattering

mediates an effective interaction between two nitrogen nuclear spins. For a specific interaction time, a universal controlled-Z (CZ) gate is implemented, which is equivalent to CNOT up to single-qubit operations. A quantitative analysis of the proposed mechanism yields gate operation times of $10 \mu\text{s}$, which is about four orders of magnitude shorter than the decoherence time of several milliseconds for the nitrogen nuclear spin. While cavity-mediated coupling between NV *electron* spins relies on the zero-field splitting [25], the coupling of NV nuclear spins has its physical origin in the hyperfine interaction.

II. MODEL

We start our analysis by describing a single NV center coupled to a single cavity mode and to an external laser field. The extension to two NV centers interacting with the same cavity mode, as required for the two-qubit gate, is straightforward and will be given later. To model the combined system of a single NV center, an optical cavity, and the external laser, we use the time-dependent Hamiltonian

$$H(t) = H_{\text{NV}} + H_c + H_L(t), \quad (1)$$

where $H_{\text{NV}} = H_e + H_n + H_{\text{hf}}$ describes the electron (e) and nuclear (n) spin systems coupled through hyperfine (hf) interactions, H_c the coupling to the cavity, and $H_L(t)$ the interaction with the laser field. In the presence of an external magnetic field $\mathbf{B} = B\mathbf{e}_z$ along the defect symmetry axis (z axis), the electron spin (\mathbf{S}) and nuclear spin (\mathbf{I}) Hamiltonians are given by ($\hbar = 1$) [25–27]

$$H_e = \gamma_e B S_z + D S_z^2 - \frac{1}{2} \Delta S_z^2 \tau_z + \frac{1}{2} E_g \tau_z, \quad (2)$$

$$H_n = -\gamma_n B I_z + Q I_z^2. \quad (3)$$

Here, $\gamma_e/2\pi = 2.803 \text{ MHz/G}$ is the electron gyromagnetic ratio, $E_g = 1.945 \text{ eV}$ is the energy gap between ground and excited state, and $D = (D_{\text{gs}} + D_{\text{es}})/2$ and $\Delta = D_{\text{gs}} - D_{\text{es}}$ with the zero-field spin splittings of the ground ($D_{\text{gs}}/2\pi = 2.88 \text{ GHz}$) and excited state ($D_{\text{es}}/2\pi = 1.42 \text{ GHz}$). The nuclear gyromagnetic ratio is denoted γ_n and Q is the nuclear electric quadrupole coupling (see Table I). To describe the

*adrian.auer@uni-konstanz.de

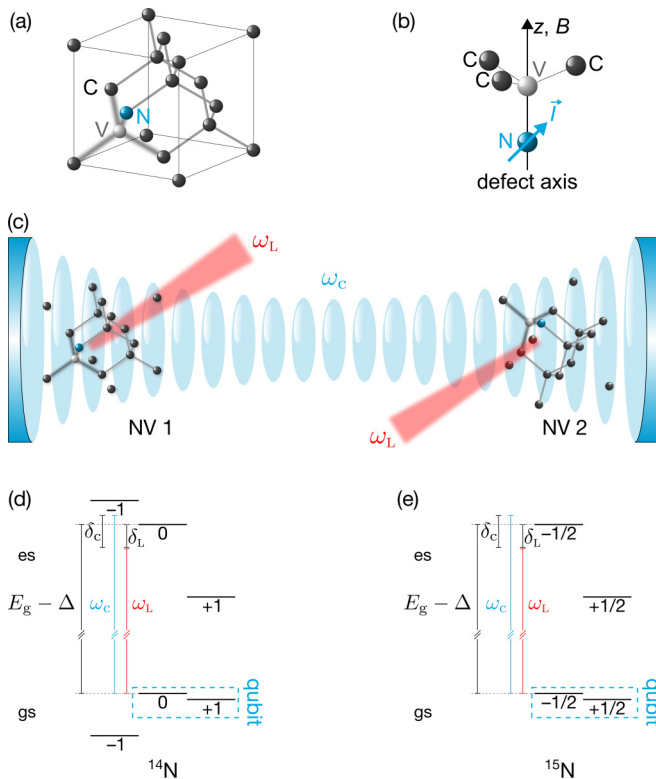


FIG. 1. (a) NV center formed by a substitutional nitrogen (N) atom next to a vacancy (V) in the diamond lattice. (b) Magnetic field (B) direction along the defect axis (z) and N nuclear spin I . (c) Interaction between two NV centers (NV 1 and NV 2) that are coupled to the same mode ω_c of an optical cavity. The NV centers are excited by two lasers of frequency ω_L . Scattering of a laser photon mediates an effective interaction between NV 1 and NV 2. (d) Hyperfine levels $m_I = 0, \pm 1$ of the $m_S = -1$ subspace for ^{14}N in the ground (gs) and excited (es) states, qubit states are indicated. δ_L and δ_c are the detunings of the laser frequency ω_L from the $m_I = 0$ orbital transition energy $E_g - \Delta$ and from the cavity frequency ω_c . (e) Hyperfine levels $m_I = \pm 1/2$ for ^{15}N .

orbital degree of freedom, we use Pauli matrices τ_i ($i = x, y, z$), and choose the ground and excited states as τ_z eigenvectors with eigenvalues -1 and $+1$, respectively. We only consider the lower orbital branch of the excited state doublet (E_y). This is justified by naturally occurring strain fields of 10 GHz and more [28], which split the excited state into two well-separated orbital branches.

Hyperfine interaction in the excited state is modeled by a diagonal hyperfine tensor, which has the same form as in the ground state [29,30]. However, since the electron density

at the nitrogen site is larger in the excited state [31], the hyperfine interaction is about 20 times stronger compared to the ground state according to measurements under ambient conditions [4,32]. The difference δA between the hyperfine coupling in the ground and the excited state forms the basis of the nuclear-spin-dependent light-scattering effect, which we predict. Working at magnetic field strengths away from the ground- and excited-state level anticrossings, electron-nuclear spin flip-flop processes are energetically suppressed. Therefore, we neglect the transverse part of the hyperfine tensor and only include the longitudinal coupling. Denoting the hyperfine coupling strengths by A_{gs} and A_{es} for the ground and excited state (Table I), we arrive at

$$H_{\text{hf}} = AS_z I_z + \frac{1}{2} \delta A \tau_z S_z I_z, \quad (4)$$

where $A = (A_{\text{es}} + A_{\text{gs}})/2$ and $\delta A = A_{\text{es}} - A_{\text{gs}}$.

We consider the NV electronic orbital transition between the ground and excited state to be coupled to a single mode of the optical cavity, which, in the rotating-wave approximation, is described by $H_c = \omega_c a^\dagger a + g(\tau_+ a + \tau_- a^\dagger)$, where ω_c is the cavity frequency, $a^{(\dagger)}$ the cavity-photon annihilation (creation) operator, g the coupling strength (which can be assumed real), and $\tau_\pm = (\tau_x \pm i\tau_y)/2$. The external laser is described by a classical field of frequency ω_L that excites electronic orbital transitions between states having the same spin projections m_S and m_I , $H_L(t) = \Omega e^{-i\omega_L t} \tau_+ + \Omega^* e^{i\omega_L t} \tau_-$. Here, Ω is the complex Rabi frequency that depends on the phase of the laser field. The Hamiltonian $H(t)$ can be made time-independent by transforming into a rotating frame, $H' = e^{i\xi t} H(t) e^{-i\xi t} - \xi$ with $\xi = \omega_c(a^\dagger a + \tau_z/2)$, and we obtain $H' = H'_e + H_n + H_{\text{hf}} + H'_c + H'_L$. The transformed part H'_e of the electronic Hamiltonian is obtained by replacing E_g with the detuning $\tilde{\delta}_L = E_g - \omega_L$ in H_c . In the Hamiltonian H'_c , the transformation causes a shift of the cavity frequency to $\delta_c = \omega_c - \omega_L$, which is the detuning of the laser from the cavity mode. The laser Hamiltonian $H_L(t)$ becomes time-independent, $H'_L = \Omega \tau_+ + \Omega^* \tau_-$.

III. NUCLEAR-SPIN DEPENDENT SCATTERING

Virtually exciting the NV center by the external laser field can finally lead to an excitation of the cavity mode through the coupling g . We describe this process by using quasidegenerate perturbation theory in terms of a Schrieffer-Wolff (SW) transformation [35,36] to eliminate the intermediate virtual transition to the excited state, and we obtain a model that effectively describes the scattering of a laser photon into the cavity mode, and vice versa, that particularly depends on the nitrogen nuclear spin projection m_I . It is exactly this spin-dependent scattering that eventually enables a conditional two-qubit quantum gate.

To implement the SW transformation, we construct an anti-Hermitian operator S such that $[S, H_0] = V$ (see Appendix B for details), where the part $H_0 = H'_e + H_n + H_{\text{hf}} + \delta_c a^\dagger a$ only acts on the ground- and excited-state manifold, respectively, and V describes transitions between these two Hilbert subspaces. In the transformed Hamiltonian $\tilde{H} = e^{-S} H' e^S$, we keep the lowest order in the interaction V and continue with the effective Hamiltonian $\tilde{H} \approx H_0 + [V, S]/2$. The effective

TABLE I. Relevant nuclear-spin parameters for the NV center.

Parameter	^{14}N	^{15}N
Nuclear spin I	1	1/2
$\gamma_n/2\pi$	0.308 kHz/G [33]	-0.432 kHz/G [33]
$Q/2\pi$	-5 MHz [1,4,34]	0
$A_{\text{gs}}/2\pi$	-2.2 MHz [1,4,5,34]	3.0 MHz [32,34]
$A_{\text{es}}/2\pi$	40 MHz [4]	61 MHz [32]

ground-state Hamiltonian becomes

$$\begin{aligned} \tilde{H}^{(\text{gs})} = & -(A_{\text{gs}} + \gamma_n B)I_z + QI_z^2 + \delta_c a^\dagger a \\ & + \frac{1}{2}[g\Omega((\delta A I_z - \delta_L)^{-1} + (\delta A I_z + \delta_c - \delta_L)^{-1})a^\dagger \\ & + \text{H.c.}], \end{aligned} \quad (5)$$

Here, we restrict our consideration to the $m_S = -1$ subspace, and define the detuning $\delta_L = \tilde{\delta}_L - \Delta$ of the laser frequency from the $m_I = 0$ orbital transition (Fig. 1). We omit all constant terms and neglect small energy shifts proportional to g^2 and $|\Omega|^2$.

On the basis of previous experimental work [3,5,15] using the ^{14}N nuclear spin as a qubit, we choose the nuclear spin sublevels $|m_I = +1\rangle = |1\rangle$ and $|m_I = 0\rangle = |0\rangle$ as the computational basis. We can neglect the $m_I = -1$ state because the transition frequency between these two levels is well separated from other transitions [5]. From Eq. (5), one can see that the effective coupling of the NV center to the cavity via the virtual laser excitation depends on the spin state of nitrogen nucleus and can, e.g., be completely suppressed for one of the two spin states. This is the case if the laser frequency is chosen such that, e.g., $\delta_L = \delta_c/2$, where only scattering from the $m_I = +1$ state is possible. By using $I_z = |1\rangle\langle 1| + |0\rangle\langle 0|$, we find the qubit Hamiltonian

$$\begin{aligned} \tilde{H}^{(\text{qubit})} = & (Q - A_{\text{gs}} - \gamma_n B)|1\rangle\langle 1| + \delta_c a^\dagger a \\ & + g'|1\rangle\langle 1|a^\dagger + (g')^*|1\rangle\langle 1|a, \end{aligned} \quad (6)$$

with an effective coupling strength

$$g' = g\Omega \frac{\delta A}{\delta A^2 - (\frac{\delta_c}{2})^2}. \quad (7)$$

Scattering only from the $m_I = 0$ state is possible for $\delta_L = \delta A + \delta_c/2$ occurring with the same effective coupling strength g' [Eq. (7)]; however, we concentrate on $m_I = +1$ scattering in the following.

IV. SPIN-SPIN INTERACTIONS

To understand the scattering mechanism of a laser photon into the cavity mode qualitatively, we so far neglected spin-mixing terms in the lower branch of the excited state doublet [26,32,37–39]. However, to make quantitative predictions of the effective scattering process, we take into account the fine structure of the excited state manifold. So far, electronic spin-spin interactions were only incorporated by the zero-field splittings D_{gs} and D_{es} . In the limit of high strain considered here, the two branches of the excited-state orbital doublet split and anticrossings in the lower branch mix spin states with different quantum numbers m_S . The Hamiltonian describing the spin mixing is [27,39]

$$H_s = \frac{1}{2}(1 + \tau_z) \left[\frac{\Delta_1}{2}(S_x^2 - S_y^2) - \frac{\Delta_2}{\sqrt{2}}(S_x S_z + S_z S_x) \right], \quad (8)$$

where transitions between the excited state orbitals have been neglected due to the high strain, and the fine structure parameters are given by $\Delta_1/2\pi = 1.54$ GHz and $\Delta_2/2\pi = 0.154$ GHz [39]. The effective coupling strength \tilde{g} analogous to Eq. (7) can be obtained by adding H_s to the bare NV Hamiltonian H_{NV} , and then performing the SW transformation.

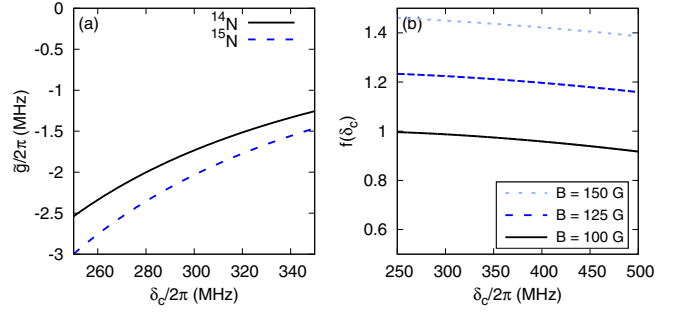


FIG. 2. (a) Effective coupling strength \tilde{g} as a function of the cavity detuning δ_c for $\Omega/2\pi = 50$ MHz, $g/2\pi = 50$ MHz, and $B = 150$ G. (b) Ratio $f(\delta_c) = \tilde{g}/g'$ of coupling strengths with (\tilde{g}) and without (g') spin-spin interaction in the excited state. Magnetic field strengths B are chosen such that m_I is a good quantum number in the ground and excited state.

In doing so, we assume the cavity to be populated by at most one photon, and only if the NV center is in the ground state. In the excited state, we need to include all spin states $m_S = 0, \pm 1$. The effective ground-state Hamiltonian in the case of $m_I = +1$ scattering has the same form as given in Eq. (6) with a different coupling strength $\tilde{g} = g'f(\delta_c)$. Explicit values for \tilde{g} and for the detuning-dependent part $f(\delta_c)$ are given in Fig. 2.

V. CONTROLLED QUANTUM GATE

For the two-qubit gate, we consider two NV centers ($i = 1, 2$) coupled to the same cavity mode and each individually driven by a laser of frequency ω_L [Fig. 1(c)] [40]. In the following, we keep only the lowest order of the interaction parts, and consider $m_I = +1$ scattering on both NV centers. Furthermore, we assume detunings δ_L and δ_c such that the cavity is excited only virtually, which, in turn, leads to an effective interaction between the two NV centers. To describe this interaction, we apply a second SW transformation to $\tilde{H}_2^{(\text{gs})} = \delta_c a^\dagger a + \sum_{i=1}^2 (Q - A_{\text{gs}} - \gamma_n B)|1\rangle_i\langle 1| + (\tilde{g}_i|1\rangle_i\langle 1|a^\dagger + \text{H.c.})$ to eliminate the cavity mode by choosing $S = -\sum_{i=1}^2 (\tilde{g}_i/\delta_c|1\rangle_i\langle 1|a^\dagger - \text{H.c.})$, which leads to an effective Hamiltonian $H_{\text{eff}} = e^{-S}\tilde{H}_2^{(\text{gs})}e^S$, where again only the lowest order contribution of the off-diagonal elements is kept (see Appendix C for details). H_{eff} comprises single-qubit terms $H_{\text{eff}}^{(i)} = (Q - A_{\text{gs}} - \gamma_n B - |\tilde{g}_i|^2/\delta_c)|1\rangle_i\langle 1|$, and a two-qubit interaction term,

$$H_{\text{int}} = -g_{12}|11\rangle\langle 11|. \quad (9)$$

Here, $|11\rangle = |1\rangle_1|1\rangle_2$ is the nuclear spin state of both NV centers 1 and 2, and the effective two-qubit coupling strength g_{12} is found to be

$$g_{12} = 2 \frac{|\tilde{g}_1||\tilde{g}_2|}{\delta_c} \cos(\phi_1 - \phi_2), \quad (10)$$

where ϕ_i denotes the phase of the i th laser field, $\Omega_i = |\Omega_i|e^{i\phi_i}$. Quantitative predictions of g_{12} are plotted in Fig. 3(a).

Since $[H_{\text{eff}}^{(i)}, H_{\text{int}}] = 0$, the time evolution U generated by the Hamiltonian H_{eff} can be written as

$$U(t) = e^{-iH_{\text{eff}}t} = [U_1(t) \otimes U_2(t)]U_{12}(t), \quad (11)$$

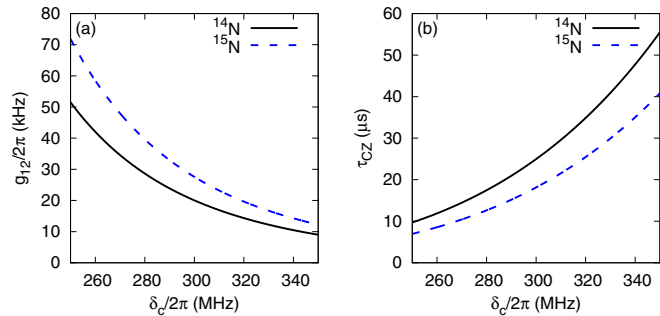


FIG. 3. (a) Effective two-qubit coupling strength g_{12} between ^{14}N and ^{15}N nuclear spins, respectively, as a function of δ_c for Rabi frequencies $\Omega_1/2\pi = \Omega_2/2\pi = 50$ MHz and cavity couplings $g_1/2\pi = g_2/2\pi = 50$ MHz. (b) Time τ_{CZ} to generate a CZ gate between the two nuclear spins as a function of δ_c using the same parameter values. All calculations performed at $B = 150$ G.

where $U_i(t)$ is a single-qubit rotation of nuclear spin i and $U_{12}(t)$ describes a two-qubit operation generated by the interaction part H_{int} . In Eq. (11), the time evolution of the cavity field has been omitted, since the nuclear spin degree of freedom has been decoupled from the cavity field by the above transformation. In the following, we only concentrate on the two-qubit interaction part, and disregard single-qubit rotations since they can be undone afterwards, e.g., by off-resonant excitation of the ground-state electronic spin transition, thereby implementing a phase gate on the N nuclear spin [5] or direct driving of the nuclear spin transitions [41].

For an operation time of $\tau_{\text{CZ}} = \pi/g_{12}$, a CZ gate is implemented on the two nuclear spin qubits,

$$U_{12}(\tau_{\text{CZ}}) = |00\rangle\langle 00| + |01\rangle\langle 01| + |10\rangle\langle 10| - |11\rangle\langle 11|, \quad (12)$$

from which CNOT can be created using additional Hadamard gates [24]. In Fig. 3(b), values of τ_{CZ} are shown for different Rabi frequencies Ω . As the main result of our paper, we find operation times below 10 μs . In our calculations, we assumed large detunings $|\delta_c| \gtrsim |g_i|$ and $|\delta_L| \gtrsim |\Omega|$ to justify the effective model used.

VI. LIMITS ON GATE FIDELITY

In this section, we identify possible mechanisms that may reduce the fidelity of the intended CZ gate. We find that finite linewidths of the excited-state hyperfine levels are the main source of fidelity reduction, and we give a detailed analysis to quantify this effect. The short lifetime of the excited state (8–12 ns [42]) and spectral diffusion due to surrounding impurities cause the excitation energy to fluctuate [43]. Especially for synthesized type Ib diamond with implanted NV centers, e.g., used to fabricate nanodiamonds, spectral diffusion becomes apparent due to a higher concentration of nitrogen impurities. However, it was demonstrated that stable excitation lines of NV centers can be observed for both type IIa bulk diamond [43,44] and synthesized type Ib diamond [45], where the linewidth is only limited by the finite lifetime of the excited state. We therefore include only the effect of lifetime broadening in our analysis, which results in a linewidth of $\Gamma \approx 13$ MHz [43,44].

The effect of finite excitation linewidths is that the nuclear-spin-dependent scattering mechanism explained in Sec. III does not work perfectly. Complete suppression of photon scattering for one of the nuclear-spin states cannot be guaranteed if the excited state has a finite linewidth and there will be some residual scattering as well if the nuclear-spin qubit is in the respective other state. Eventually, this effect leads to the implementation of a nonperfect CZ gate, for which we quantify the fidelity in the following.

In general, the Hamiltonian $\tilde{H}_2^{(\text{gs})}$ contains scattering matrix elements $\eta_\nu^{(i)}$ for both qubit states $\nu = 0$ and 1,

$$\begin{aligned} \tilde{H}_2^{(\text{gs})} = & \delta_c a^\dagger a + \sum_{i=1}^2 (Q - A_{\text{gs}} - \gamma_n B) |1\rangle_i \langle 1| \\ & + (\eta_1^{(i)} |1\rangle_i \langle 1| a^\dagger + \eta_0^{(i)} |0\rangle_i \langle 0| a^\dagger + \text{H.c.}). \end{aligned} \quad (13)$$

We incorporate finite excited-state linewidths by assuming the scattering matrix elements to depend on the laser detuning independently, i.e.,

$$\eta_\nu^{(i)} \equiv \eta_\nu^{(i)}(\delta_{L,\nu}^{(i)}), \quad (14)$$

because the detuning $\delta_{L,\nu}^{(i)}$ of the i th laser from the respective optical transition energies varies independently for each transition. The line shape of the excited-state levels directly transforms into a probabilistic distribution of laser detunings, for which we assume a Lorentzian probability density function of the form [4,32,43–46]

$$p(\delta_{L,\nu}^{(i)}) = \frac{1}{\pi} \frac{\frac{\Gamma}{2}}{(\delta_{L,\nu}^{(i)} - \bar{\delta})^2 + (\frac{\Gamma}{2})^2}, \quad (15)$$

where Γ denotes the linewidth and $\bar{\delta}$ the mean detuning, assumed to be equally large for each transition. One obtains perfect suppression of scattering for one of the nuclear spin states if the detuning is equal to $\bar{\delta}$ and therefore a perfect CZ gate; i.e., we have $\eta_0^{(i)}(\bar{\delta}) = 0$, which corresponds to the case discussed before. Following the procedure given in Sec. V, we eventually obtain a different two-qubit operation $U'_{12}(\tau_{\text{CZ}}, \{\delta_{L,\nu}^{(i)}\})$ for finite deviations $\delta_{L,\nu}^{(i)}$ from the mean value $\bar{\delta}$ after the same operation time τ_{CZ} .

The fidelity F of the actually implemented quantum gate with respect to a perfect CZ gate $U_{\text{CZ}} \equiv U_{12}(\tau_{\text{CZ}})$ is quantified via [47]

$$F(\{\delta_{L,\nu}^{(i)}\}) = \frac{4 + |\text{Tr}[U_{\text{CZ}}^\dagger U'_{12}(\tau_{\text{CZ}}, \{\delta_{L,\nu}^{(i)}\})]|^2}{20}. \quad (16)$$

To include the effect of finite linewidths, we calculate an average fidelity,

$$\bar{F} = \int \left(\prod_{i,\nu} d\delta_{L,\nu}^{(i)} p(\delta_{L,\nu}^{(i)}) \right) F(\{\delta_{L,\nu}^{(i)}\}). \quad (17)$$

The averaging process is performed numerically by choosing a set of random values for the four detunings that are distributed according to Eq. (15) and then calculating the fidelity for those values. We find that averaging over a sufficiently large number of such sets of detunings leads to good convergence of the average. For our proposed gate mechanism, one can still

achieve fidelities that are larger than 91 (92)% for ^{14}N (^{15}N) nuclear spins, including the finite linewidth of the excited state.

An increase in fidelity could be achieved by using NV centers with longer excited-state lifetimes and therefore smaller linewidths. Recent studies on NV centers in nanodiamonds showed increased excited-state lifetimes between 16 and 29 ns [48]. Provided that those NV centers exhibit a stable excitation line [45], increased average fidelities up to 96 (97)% for ^{14}N (^{15}N) nuclear spins could be achieved for the longest lifetime of 29 ns.

We estimate level broadening to be the main source of gate errors. The probability for cavity loss is $p_{\text{loss}} \approx (|\tilde{g}_i|/\delta_c)^2(1 - e^{-\kappa t}) \approx (|\tilde{g}_i|/\delta_c)^2$, where κ is the cavity-loss rate and $(|\tilde{g}_i|/\delta_c)^2 \lesssim 0.04\%$ is the probability for cavity population by a single photon for parameter values used previously. If we assume perfect fidelity if no photon is emitted and zero fidelity if the photon is lost, the average fidelity with respect to this mechanism is $1 - p_{\text{loss}}$ and we can thus neglect cavity decay. Another source of errors is spontaneous emission from the excited states. The probability for populating the excited state is $(|\Omega|/\delta_L)^2 \lesssim 1\%$, and for the same reasoning as before we can also neglect fidelity loss due to spontaneous emission.

VII. CONCLUSIONS

Nitrogen nuclear spins in diamond have proved to be highly promising candidates to physically realize qubits. We have presented a theoretical proposal for the implementation of a controlled optical cavity-mediated quantum gate between two nitrogen nuclear spin qubits intrinsic to NV centers in diamond. The robustness of two-qubit gates that are generated by an effective interaction using an optical cavity has been demonstrated in previous works, e.g., for NV center electron spins [25,49–53].

The derived scheme requires lifetime-limited line broadening in the excited state and therefore works at low temperatures. Gate operation can be achieved within $10 \mu\text{s}$ or less, which is about four orders of magnitude below the nuclear-spin decoherence time. Our proposal requires the interaction between a NV center and an optical cavity to be in the strong coupling regime of cavity QED. Using whispering gallery modes of silica microsphere cavities with large quality factors (about 10^8), it has been demonstrated experimentally that single NV centers can be strongly coupled to cavities. Further progress in the development of optical cavities exceeding quality factors of 10^5 has recently been achieved for photonic crystal cavities in bulk diamond [54], which are promising elements of diamond-based nanophotonics [55,56].

In addition to the presented findings, an equivalent analysis for the ^{15}N nuclear spin with $I = 1/2$ shows that the proposed scheme also works for this isotope if the computational basis is chosen as $|1\rangle = |m_I = +1/2\rangle$ and $|0\rangle = |m_I = -1/2\rangle$ [Fig. 1(e)]. We find the same effective scattering rate g' [Eq. (7)] for $m_I = \pm 1/2$ scattering for laser detunings $\delta_L = (\delta_c \mp \delta A)/2$. Including spin-spin interactions, the effective two-qubit coupling strength g_{12} and the gate time τ_{CZ} show qualitatively the same behavior as for the ^{14}N nuclear spin, and are also depicted in Fig. 3.

During the fast electronic excitation cycles, the nuclear spins are subject to a time-varying hyperfine interaction.

However, it has been shown that the effect on the nuclear-spin coherence is negligibly small and coherence can be preserved in the presence of incoherent spontaneous emission processes from the NV center excited state [12,57]. Together with elementary and experimentally demonstrated single-qubit operations, the realization of a universal CZ gate makes the nitrogen nuclear spin valuable for quantum computation in addition to its remarkable quality as a quantum memory [15].

ACKNOWLEDGMENTS

We acknowledge funding from the DFG within SFB 767 and from the BMBF under the program Q.com-HL.

APPENDIX A: NV CENTER HAMILTONIAN

The form of the NV center Hamiltonian H_{NV} [Eqs. (2)–(4)] can be obtained from the known 3A_2 ground and 3E excited-state Hamiltonians. The ground state (gs) of a single NV center is described by the Hamiltonian H_{gs} [26,27,38],

$$H_{\text{gs}} = D_{\text{gs}} S_z^2 + \gamma_e \mathbf{B} \cdot \mathbf{S} - \gamma_n \mathbf{B} \cdot \mathbf{I} + A_{\text{gs}}^\perp (S_x I_x + S_y I_y) + A_{\text{gs}}^\parallel S_z I_z + Q I_z^2. \quad (\text{A1})$$

Here \mathbf{S} and \mathbf{I} denote the electron and nuclear spin, respectively. D_{gs} is the zero-field splitting separating the $m_S = 0$ state from the $m_S = \pm 1$ states at zero magnetic field, $\gamma_{e(n)}$ is the electron (nuclear) gyromagnetic ratio, and Q the nuclear electric quadrupole coupling. Hyperfine interaction in the ground state is described by a transversal (A_{gs}^\perp) and longitudinal (A_{gs}^\parallel) part. However, we assume magnetic field strengths that are sufficiently far away from the ground-state level anticrossing such that the energy splitting of the electron-spin states is much larger than the transversal component of the hyperfine tensor A_{gs}^\perp and therefore, electron-nuclear spin flip-flop processes are energetically suppressed. The terms proportional to A_{gs}^\perp can thus be neglected in our description and we denote $A_{\text{gs}}^\parallel \equiv A_{\text{gs}}$.

We model hyperfine interaction in the excited state as well through a diagonal hyperfine tensor of a form equivalent to the ground state [29,30]. Accordingly, the excited-state Hamiltonian H_{es} has the same structure as the ground-state Hamiltonian,

$$H_{\text{es}} = D_{\text{es}} S_z^2 + \gamma_e \mathbf{B} \cdot \mathbf{S} - \gamma_n \mathbf{B} \cdot \mathbf{I} + A_{\text{es}}^\perp (S_x I_x + S_y I_y) + A_{\text{es}}^\parallel S_z I_z + Q I_z^2, \quad (\text{A2})$$

where additional terms originating from spin-spin interactions (see Sec. IV) are so far not included but are taken into account for quantitative analyses. Spin states are also split in the excited state by a different zero-field splitting D_{es} and the hyperfine coupling constants are different due to a redistribution of electron density in the excited state [4,31,32]. We neglect transversal hyperfine coupling by assuming magnetic field strengths also sufficiently far away from the excited-state level anticrossing and denote $A_{\text{es}}^\parallel \equiv A_{\text{es}}$ in the main text.

To use a single Hamiltonian for the NV center, we introduce Pauli matrices τ_i ($i = x, y, z$) that operate on the orbital degree

of freedom [25], i.e.,

$$\tau_z|es\rangle = |es\rangle, \quad (\text{A3})$$

$$\tau_z|gs\rangle = -|gs\rangle, \quad (\text{A4})$$

and $|gs\rangle$ ($|es\rangle$) denotes the electronic orbital ground (excited) state. The Hamiltonian H_{NV} of a single NV center is thus given by

$$\begin{aligned} H_{\text{NV}} &= \frac{1}{2}(1 - \tau_z)H_{\text{gs}} + \frac{1}{2}(1 + \tau_z)(H_{\text{es}} + E_{\text{g}}) \\ &= H_{\text{e}} + H_{\text{n}} + H_{\text{hf}} + \frac{1}{2}E_{\text{g}}, \end{aligned} \quad (\text{A5})$$

where E_{g} denotes the transition energy between the ground and excited state. The Hamiltonian H_{NV} obtains the form given in the main text by assuming a magnetic field along the defect symmetry axis, i.e., $\mathbf{B} = B\mathbf{e}_z$, and by neglecting the constant energy shift $E_{\text{g}}/2$ in Eq. (A5).

APPENDIX B: SCHRIEFER-WOLFF TRANSFORMATION TO ELIMINATE EXCITED STATE

We separate the Hamiltonian H' into a block-diagonal part H_0 that only acts within the ground- and the excited-state manifold, respectively, and an off-diagonal part V that connects these two manifolds,

$$H' = H_0 + V. \quad (\text{B1})$$

To implement the Schrieffer-Wolff (SW) transformation [35,36], we construct a unitary transformation $\exp(-S)$ with some anti-Hermitian matrix S to obtain a new Hamiltonian \tilde{H} ,

$$\tilde{H} = e^{-S}H'e^S, \quad (\text{B2})$$

which contains no matrix elements that connect the ground and the excited states up to a desired order in V . If we choose the anti-Hermitian operator S in such a way that

$$[S, H_0] = V \quad (\text{B3})$$

holds, the leading order in V cancels. If we keep the lowest order in V , the Hamiltonian \tilde{H} is approximately given by

$$\tilde{H} \approx H_0 + \frac{1}{2}[V, S]. \quad (\text{B4})$$

The block-diagonal part H_0 of H' is given by

$$H_0 = H'_{\text{e}} + H_{\text{n}} + H_{\text{hf}} + \delta_{\text{c}}a^\dagger a, \quad (\text{B5})$$

and the interaction terms are

$$V = g(\tau_+ a + \tau_- a^\dagger) + \Omega\tau_+ + \Omega^*\tau_-. \quad (\text{B6})$$

From the condition in Eq. (B3), we find

$$\begin{aligned} S &= \Omega(\Delta S_z^2 - \Delta_{\text{hf}}S_z I_z - \tilde{\delta}_{\text{L}})^{-1}\tau_+ - \text{H.c.} \\ &+ g(\Delta S_z^2 - \Delta_{\text{hf}}S_z I_z + \delta_{\text{c}} - \tilde{\delta}_{\text{L}})^{-1}\tau_+ a - \text{H.c.}, \end{aligned} \quad (\text{B7})$$

and the effective Hamiltonian for the decoupled ground-state manifold becomes

$$\begin{aligned} \tilde{H}^{(\text{gs})} &= -(A_{\text{gs}} + \gamma_{\text{n}}B)I_z + QI_z^2 + \delta_{\text{c}}a^\dagger a \\ &+ \frac{1}{2}[g\Omega((\Delta_{\text{hf}}I_z - \delta_{\text{L}})^{-1} \\ &+ (\Delta_{\text{hf}}I_z + \delta_{\text{c}} - \delta_{\text{L}})^{-1})a^\dagger + \text{H.c.}]. \end{aligned} \quad (\text{B8})$$

Here, we restrict our consideration to the $m_S = -1$ subspace, and define the detuning $\delta_{\text{L}} = \tilde{\delta}_{\text{L}} - \Delta$ of the laser frequency from the $m_I = 0$ orbital transition. We omit all constant terms and neglect small energy shifts proportional to g^2 and $|\Omega|^2$.

APPENDIX C: SW TRANSFORMATION TO ELIMINATE VIRTUAL PHOTON

We start from a Hamiltonian $\tilde{H}_2^{(\text{gs})}$ that describes two NV centers ($i = 1, 2$) coupled to a common cavity mode and each driven by a laser of frequency ω_{L} ,

$$\begin{aligned} \tilde{H}_2^{(\text{gs})} &= \delta_{\text{c}}a^\dagger a + \sum_{i=1}^2 (Q - A_{\text{gs}} - \gamma_{\text{n}}B)|1\rangle_i \langle 1| \\ &+ \tilde{g}_i|1\rangle_i \langle 1|a^\dagger + \tilde{g}_i^*|1\rangle_i \langle 1|a, \end{aligned} \quad (\text{C1})$$

where we consider $m_I = +1$ scattering on both NV centers and assume detunings δ_{L} and δ_{c} , such that the cavity is excited only virtually. The effective coupling strength \tilde{g}_i is given by

$$\tilde{g}_i = g'_i f(\delta_{\text{c}}) = g_i \Omega_i \frac{\delta A}{\delta A^2 - (\frac{\delta_{\text{c}}}{2})^2} f(\delta_{\text{c}}), \quad (\text{C2})$$

where g_i is the coupling strength of NV center i to the cavity and Ω_i is the Rabi frequency of the i th laser field.

To derive an effective interaction between the two nuclear spin qubits, we apply a second SW transformation to eliminate the cavity mode, i.e., to decouple the subspaces containing zero and one cavity photon, by choosing

$$S = - \sum_{i=1}^2 \left(\frac{\tilde{g}_i}{\delta_{\text{c}}} |1\rangle_i \langle 1| a^\dagger - \text{H.c.} \right). \quad (\text{C3})$$

We obtain an effective Hamiltonian through the unitary transformation

$$H_{\text{eff}} = e^{-S} \tilde{H}_2^{(\text{gs})} e^S \approx \sum_{i=1}^2 H_{\text{eff}}^{(i)} + H_{\text{int}} + \delta_{\text{c}}a^\dagger a, \quad (\text{C4})$$

where we also keep terms up to the lowest order in the off-diagonal matrix elements. The Hamiltonian H_{eff} contains terms that only act on a single nuclear spin i ,

$$H_{\text{eff}}^{(i)} = \left(Q - A_{\text{gs}} - \gamma_{\text{n}}B - \frac{|\tilde{g}_i|^2}{\delta_{\text{c}}} \right) |1\rangle_i \langle 1|, \quad (\text{C5})$$

and an interaction part H_{int} that couples the two nuclear spin qubits,

$$H_{\text{int}} = -g_{12}|11\rangle \langle 11|. \quad (\text{C6})$$

The last term in Eq. (C4) is zero in the considered subspace that contains no photons.

- [1] B. Smeltzer, J. McIntyre, and L. Childress, *Phys. Rev. A* **80**, 050302 (2009).
- [2] F. Jelezko, T. Gaebel, I. Popa, M. Domhan, A. Gruber, and J. Wrachtrup, *Phys. Rev. Lett.* **93**, 130501 (2004).
- [3] W. Pfaff, T. H. Taminiau, L. Robledo, H. Bernien, M. Markham, D. J. Twitchen, and R. Hanson, *Nat. Phys.* **9**, 29 (2013).
- [4] M. Steiner, P. Neumann, J. Beck, F. Jelezko, and J. Wrachtrup, *Phys. Rev. B* **81**, 035205 (2010).
- [5] S. Sangtawesin, T. O. Brundage, and J. R. Petta, *Phys. Rev. Lett.* **113**, 020506 (2014).
- [6] S. Sangtawesin and J. R. Petta, [arXiv:1503.07464](https://arxiv.org/abs/1503.07464).
- [7] V. Jacques, P. Neumann, J. Beck, M. Markham, D. Twitchen, J. Meijer, F. Kaiser, G. Balasubramanian, F. Jelezko, and J. Wrachtrup, *Phys. Rev. Lett.* **102**, 057403 (2009).
- [8] P. Neumann, J. Beck, M. Steiner, F. Rempp, H. Fedder, P. R. Hemmer, J. Wrachtrup, and F. Jelezko, *Science* **329**, 542 (2010).
- [9] L. Robledo, L. Childress, H. Bernien, B. Hensen, P. F. A. Alkemade, and R. Hanson, *Nature* **477**, 574 (2011).
- [10] A. Dréau, P. Spinicelli, J. R. Maze, J.-F. Roch, and V. Jacques, *Phys. Rev. Lett.* **110**, 060502 (2013).
- [11] G. Waldherr, Y. Wang, S. Zaiser, M. Jamali, T. Schulte-Herbruggen, H. Abe, T. Ohshima, J. Isoya, J. F. Du, P. Neumann, and J. Wrachtrup, *Nature* **506**, 204 (2014).
- [12] M. V. G. Dutt, L. Childress, L. Jiang, E. Togan, J. Maze, F. Jelezko, A. S. Zibrov, P. R. Hemmer, and M. D. Lukin, *Science* **316**, 1312 (2007).
- [13] L. Jiang, J. S. Hodges, J. R. Maze, P. Maurer, J. M. Taylor, D. G. Cory, P. R. Hemmer, R. L. Walsworth, A. Yacoby, A. S. Zibrov, and M. D. Lukin, *Science* **326**, 267 (2009).
- [14] T. van der Sar, Z. H. Wang, M. S. Blok, H. Bernien, T. H. Taminiau, D. M. Toyli, D. A. Lidar, D. D. Awschalom, R. Hanson, and V. V. Dobrovitski, *Nature* **484**, 82 (2012).
- [15] G. D. Fuchs, G. Burkard, P. V. Klimov, and D. D. Awschalom, *Nat. Phys.* **7**, 789 (2011).
- [16] P. Neumann, N. Mizuochi, F. Rempp, P. Hemmer, H. Watanabe, S. Yamasaki, V. Jacques, T. Gaebel, F. Jelezko, and J. Wrachtrup, *Science* **320**, 1326 (2008).
- [17] F. Dolde, I. Jakobi, B. Naydenov, N. Zhao, S. Pezzagna, C. Trautmann, J. Meijer, P. Neumann, F. Jelezko, and J. Wrachtrup, *Nat. Phys.* **9**, 139 (2013).
- [18] F. Dolde, V. Bergholm, Y. Wang, I. Jakobi, B. Naydenov, S. Pezzagna, J. Meijer, F. Jelezko, P. Neumann, T. Schulte-Herbruggen, J. Biamonte, and J. Wrachtrup, *Nat. Commun.* **5**, 3371 (2014).
- [19] T. H. Taminiau, J. Cramer, T. van der Sar, V. V. Dobrovitski, and R. Hanson, *Nat. Nanotech.* **9**, 171 (2014).
- [20] L. Childress, J. M. Taylor, A. S. Sørensen, and M. D. Lukin, *Phys. Rev. A* **72**, 052330 (2005).
- [21] L. Childress, J. M. Taylor, A. S. Sørensen, and M. D. Lukin, *Phys. Rev. Lett.* **96**, 070504 (2006).
- [22] A. Bermudez, F. Jelezko, M. B. Plenio, and A. Retzker, *Phys. Rev. Lett.* **107**, 150503 (2011).
- [23] K. Nemoto, M. Trupke, S. J. Devitt, A. M. Stephens, B. Scharfenberger, K. Buczak, T. Nöbauer, M. S. Everitt, J. Schmiedmayer, and W. J. Munro, *Phys. Rev. X* **4**, 031022 (2014).
- [24] M. A. Nielsen and I. L. Chuang, *Quantum Computation and Quantum Information* (Cambridge University Press, Cambridge, 2000).
- [25] G. Burkard and D. D. Awschalom, [arXiv:1402.6351](https://arxiv.org/abs/1402.6351).
- [26] M. W. Doherty, N. B. Manson, P. Delaney, and L. C. L. Hollenberg, *New J. Phys.* **13**, 025019 (2011).
- [27] M. W. Doherty, N. B. Manson, P. Delaney, F. Jelezko, J. Wrachtrup, and L. C. Hollenberg, *Phys. Rep.* **528**, 1 (2013).
- [28] V. Dobrovitski, G. Fuchs, A. Falk, C. Santori, and D. Awschalom, *Annu. Rev. Condens. Matter Phys.* **4**, 23 (2013).
- [29] A. Gali, *Phys. Rev. B* **80**, 241204 (2009).
- [30] V. Ivády, K. Szász, A. L. Falk, P. V. Klimov, D. J. Christle, E. Jánzén, I. A. Abrikosov, D. D. Awschalom, and A. Gali, *Phys. Rev. B* **92**, 115206 (2015).
- [31] A. Gali, M. Fyta, and E. Kaxiras, *Phys. Rev. B* **77**, 155206 (2008).
- [32] G. D. Fuchs, V. V. Dobrovitski, R. Hanson, A. Batra, C. D. Weis, T. Schenkel, and D. D. Awschalom, *Phys. Rev. Lett.* **101**, 117601 (2008).
- [33] R. K. Harris, E. D. Becker, S. M. Cabral de Menzes, R. Goodfellow, and P. Granger, *Pure Appl. Chem.* **73**, 1795 (2001).
- [34] S. Felton, A. M. Edmonds, M. E. Newton, P. M. Martineau, D. Fisher, D. J. Twitchen, and J. M. Baker, *Phys. Rev. B* **79**, 075203 (2009).
- [35] J. R. Schrieffer and P. A. Wolff, *Phys. Rev.* **149**, 491 (1966).
- [36] R. Winkler, in *Spin–Orbit Coupling Effects in Two-Dimensional Electron and Hole Systems*, Springer Tracts in Modern Physics, Vol. 191 (Springer, Berlin, 2003), pp. 201–206.
- [37] A. Batalov, V. Jacques, F. Kaiser, P. Siyushev, P. Neumann, L. J. Rogers, R. L. McMurtrie, N. B. Manson, F. Jelezko, and J. Wrachtrup, *Phys. Rev. Lett.* **102**, 195506 (2009).
- [38] J. R. Maze, A. Gali, E. Togan, Y. Chu, A. Trifonov, E. Kaxiras, and M. D. Lukin, *New J. Phys.* **13**, 025025 (2011).
- [39] L. C. Bassett, F. J. Heremans, D. J. Christle, C. G. Yale, G. Burkard, B. B. Buckley, and D. D. Awschalom, *Science* **345**, 1333 (2014).
- [40] For simplicity, we assume equal laser frequencies, such that the coupling could in principle be realized using a single laser. However, the strain environments of the two NV centers are usually different, which would require different excitation frequencies and therefore two laser fields.
- [41] M. S. Everitt, S. Devitt, W. J. Munro, and K. Nemoto, *Phys. Rev. A* **89**, 052317 (2014).
- [42] A. Batalov, C. Zierl, T. Gaebel, P. Neumann, I.-Y. Chan, G. Balasubramanian, P. R. Hemmer, F. Jelezko, and J. Wrachtrup, *Phys. Rev. Lett.* **100**, 077401 (2008).
- [43] Kai-Mei C. Fu, C. Santori, P. E. Barclay, L. J. Rogers, N. B. Manson, and R. G. Beausoleil, *Phys. Rev. Lett.* **103**, 256404 (2009).
- [44] P. Tamarat, T. Gaebel, J. R. Rabeau, M. Khan, A. D. Greentree, H. Wilson, L. C. L. Hollenberg, S. Praver, P. Hemmer, F. Jelezko, and J. Wrachtrup, *Phys. Rev. Lett.* **97**, 083002 (2006).
- [45] Y. Shen, T. M. Sweeney, and H. Wang, *Phys. Rev. B* **77**, 033201 (2008).
- [46] J. Wrachtrup and F. Jelezko, *J. Phys. Condens. Matter* **18**, S807 (2006).
- [47] L. H. Pedersen, N. M. Møller, and K. Mølmer, *Phys. Lett. A* **367**, 47 (2007).

- [48] J. Storteboom, P. Dolan, S. Castelletto, X. Li, and M. Gu, *Opt. Express* **23**, 11327 (2015).
- [49] W. L. Yang, Z. Q. Yin, Z. Y. Xu, M. Feng, and J. F. Du, *Appl. Phys. Lett.* **96**, 241113 (2010).
- [50] W. Yang, Z. Xu, M. Feng, and J. Du, *New J. Phys.* **12**, 113039 (2010).
- [51] Q. Chen, W. Yang, M. Feng, and J. Du, *Phys. Rev. A* **83**, 054305 (2011).
- [52] P.-B. Li, S.-Y. Gao, and F.-L. Li, *Phys. Rev. A* **83**, 054306 (2011).
- [53] P.-B. Li, S.-Y. Gao, H.-R. Li, S.-L. Ma, and F.-L. Li, *Phys. Rev. A* **85**, 042306 (2012).
- [54] M. J. Burek, Y. Chu, M. S. Z. Liddy, P. Patel, J. Rochman, S. Meesala, W. Hong, Q. Quan, M. D. Lukin, and M. Lončar, *Nat. Commun.* **5**, 5718 (2014).
- [55] I. Aharonovich, A. D. Greentree, and S. Prawer, *Nat. Photon.* **5**, 397 (2011).
- [56] B. J. M. Hausmann, J. T. Choy, T. M. Babinec, B. J. Shields, I. Bulu, M. D. Lukin, and M. Lončar, *Phys. Status Solidi A* **209**, 1619 (2012).
- [57] L. Jiang, M. V. G. Dutt, E. Togan, L. Childress, P. Cappellaro, J. M. Taylor, and M. D. Lukin, *Phys. Rev. Lett.* **100**, 073001 (2008).